Fitness Trade-Offs Lead to Suppressor Tolerance in Yeast

Article *in* Molecular Biology and Evolution · October 2016

DOI: 10.1093/molbev/msw225

2 authors:

Jing Hou
University of Toronto
15 PUBLICATIONS **97** CITATIONS
SEE PROFILE

Joseph Schacherer
University of Strasbourg
58 PUBLICATIONS **1,089** CITATIONS
SEE PROFILE

Fitness Trade-Offs Lead to Suppressor Tolerance in Yeast

Jing Hou and Joseph Schacherer*
Department of Genetics, Genomics and Microbiology, University of Strasbourg, Strasbourg, France
*Corresponding author: E-mail: schacherer@unistra.fr.

Associate editor: Nicole Perna
Data deposition: Short reads data associated with this study have been uploaded to the European Nucleotide Archive (ENA) under the accession number PRJEB14235.

Abstract

Genetic variation among individuals within a population provides the raw material for phenotypic diversity upon which natural selection operates. Some given variants can act on multiple standing genomic variations simultaneously and release previously inaccessible phenotypes, leading to increased adaptive potential upon challenging environments. Previously, we identified such a variant related to a tRNA nonsense suppressor in yeast. When introduced into other genetic backgrounds, the suppressor led to an increased population phenotypic variance on various culture conditions, conferring background and environment specific selective advantages. Nonetheless, most isolates are intolerant to the suppressor on rich media due to a severe fitness cost. Here, we found that the tolerance to suppressor is related to a surprising level of fitness outburst, showing a trade-off effect to accommodate the cost of carrying the suppressor. To dissect the genetic basis of such trade-offs, we crossed strains with contrasting tolerance levels on rich media, and analyzed the fitness distribution patterns in the offspring. Combining quantitative tetrad analysis and bulk segregant analysis, we identified two genes, namely *MKT1* and *RGA1*, involved in suppressor tolerance. We showed that alleles from the tolerant parent for both genes conferred a significant gain of fitness, which increased the suppressor tolerance. Our results present a detailed dissection of suppressor tolerance in yeast and provide insights into the molecular basis of trade-offs between fitness and evolutionary potential.

Key words: **evolutionary capacitance, fitness trade-offs, natural variation, yeast.**

Article

Introduction

Natural isolates of the yeast *Saccharomyces cerevisiae* are genetically diverse and display significant phenotypic heterogeneity when challenged by external stresses (Warringer et al. 2011; Skelly et al. 2013; Bergstrom et al. 2014). Many mechanisms, including point mutations (Fay 2013; Skelly et al. 2013), copy number variations (Dunham et al. 2002; Gresham et al. 2008) and large-scale chromosomal changes (Yona et al. 2012; Chang et al. 2013) can be involved in direct response to stressful environments (Fay 2013). Interestingly, instead of specific response to a given type of stress, a particular mechanism, known as evolutionary capacitance, allows for simultaneous revelation of preexisting conditionally neutral genetic variants, which leads to increased adaptive potential (Halfmann et al. 2010). An extensively studied example of evolutionary capacitor is the yeast prion [PSI^+], related to conformational switch of the translation termination factor Sup35p (True and Lindquist 2000; Halfmann et al. 2012). When switched to prion form, Sup35p aggregates into amyloid, resulting in reduced termination efficiency and stop codon read-through (True and Lindquist 2000; Torabi and Kruglyak 2012). Depending on different genomic contexts, [PSI^+] could generate proteomic novelties that may be advantageous in fluctuating environments (Halfmann et al. 2012).

In addition to prions, we previously identified a UAA (ochre) suppressor *SUP7* originated from a mutation in a tyrosine tRNA tY(GUA)J1 in a clinical isolate YJM421, which could also act as an evolutionary capacitor with effects similar to that of [PSI^+] (Hou et al. 2015). Curiously, compared with prions, the frequency of tRNA suppressors across natural population of yeast is exceedingly low. Across more than 100 sequenced *S. cerevisiae* isolates to date (Strope et al. 2015), the *SUP7* allele was the only tRNA suppressor of any stop codon class identified so far (Hou et al. 2015). One possible explanation is that carrying such suppressors may impose a fitness cost, presumably due to excessive read-through of native stop codons leading to internal proteomic stress (True and Lindquist 2000; Torabi and Kruglyak 2012). Indeed, it has been shown in laboratory strains that individuals carrying highly efficient amber or ochre suppressors displayed poor growth on rich media, the effect of which may be alleviated by subsequent loss of the suppressor (Liebman and Sherman 1976). Nevertheless, in exception of a few lab strains, the fitness consequences of carrying a tRNA suppressor were unknown in most natural genetic backgrounds.

By introducing *SUP7* into a large number of diverse natural isolates, we previously observed an increased phenotypic variance at the population level in the presence of a large number of stress conditions, indicating that the suppressor can act as an evolutionary capacitor and may confer context specific selective advantages. However, most isolates displayed significant fitness loss due to the suppressor, with a maximum of >2.5-folds of reduced growth on rich media (Hou et al. 2015).

Interestingly, the original isolate YJM421 does not show any apparent fitness defect compared with other isolates, indicating that this strain might be intrinsically adapted to the presence of the suppressor.

The YJM421 isolate therefore offers an opportunity to dissect the basis of tolerance to tRNA suppressor and proteomic stress. In YJM421, the *SUP7* allele is expressed and functional, as indicated by the active suppression of a TAA nonsense mutation in the *COX15* gene (*cox15*^{stop}) specific to YJM421 (Hou et al. 2015). *COX15* encodes for a mitochondrial transmembrane cargo protein, the function of which is essential for respiration. In the absence of *SUP7*, the *cox15*^{stop}allele is translated to a truncate protein leading to respiratory deficiency. The fact that YJM421 is respiratory competent indicates that *SUP7* is expressed, therefore the suppressor tolerance in this particular background was not due to lack of suppressor activity. Instead, other molecular mechanisms may be involved.

Here, to understand the genetic basis of suppressor tolerance, we performed multiple crosses using allelic variants of YJM421 and a laboratory reference strain S288c, previously shown to be sensitive to the suppressor (Hou et al. 2015). By analyzing the fitness effects and distribution patterns across progeny from different parental combinations, we showed that the suppressor tolerance was related to a surprising level of fitness outburst due to variation in the YJM background. In fact, when *SUP7* is absent, the YJM strain displayed an abnormally high level of fitness, which could potentially present a trade-off to accommodate the cost of carrying the suppressor. Using bulk segregant analysis, we identified two candidate genes *MKT1* and *RGA1*, the effects of which were then validated using allele replacements. We showed that the YJM alleles of both *MKT1* and *RGA1* contribute to the observed high level of fitness, possibly due to dysregulation of the cellular energy homeostasis. Our results provide interesting insights into the molecular basis of trade-offs between fitness and evolutionary potential.

Results

Suppressor-Related Fitness Transgression in Hybrid Backgrounds

To understand the genetic basis of the observed suppressor tolerance, we crossed YJM421 (hereinafter YJM) with S288c (hereinafter FY), a laboratory strain with marked fitness cost in the presence of the suppressor on rich media (Hou et al. 2015). Meiotic offspring from the resulting hybrid were generated, and the fitness of each individual was measured as the colony size appeared 48 h after tetrad dissection. The fitness of the parental strains was measured by dissecting the corresponding homozygous diploids using the same strategy. We used exponentially growing haploid FY cells as intra-plate controls, where the single cell fitness value for each tested individual corresponds to the observed colony size normalized with the control. In all cases, only full tetrads (*i.e.* containing four viable spores) were considered (fig. 1). Using this strategy, we obtained accurate single cell fitness estimations for a large number of segregants from either homozygous or hybrid backgrounds (fig. 1A). Compared with FY, the YJM strain showed no fitness differences despite of carrying a suppressor (fig. 1A). However, progeny originated from the FY/YJM hybrid displayed significant fitness transgression, indicating that the tolerance to suppressor is genetically complex.

In addition to the suppressor, the YJM strain also carries a *cox15*^{stop} allele with a premature TAA stop codon, which is actively suppressed by *SUP7* (Hou et al. 2015). As the function of *COX15* is essential for respiration, offspring from the FY/YJM hybrid inheriting the *cox15*^{stop} allele without the suppressor would result in respiratory deficiency and "petite" colony morphology. To test the effect of *cox15*^{stop}on the observed fitness transgression, we generated a variant of the YJM background with *cox15*^{stop} replaced by the functional version of FY. The resulting strain Y22 (*COX15/SUP7*) was crossed with FY (fig. 1B). We observed no fitness effect related to

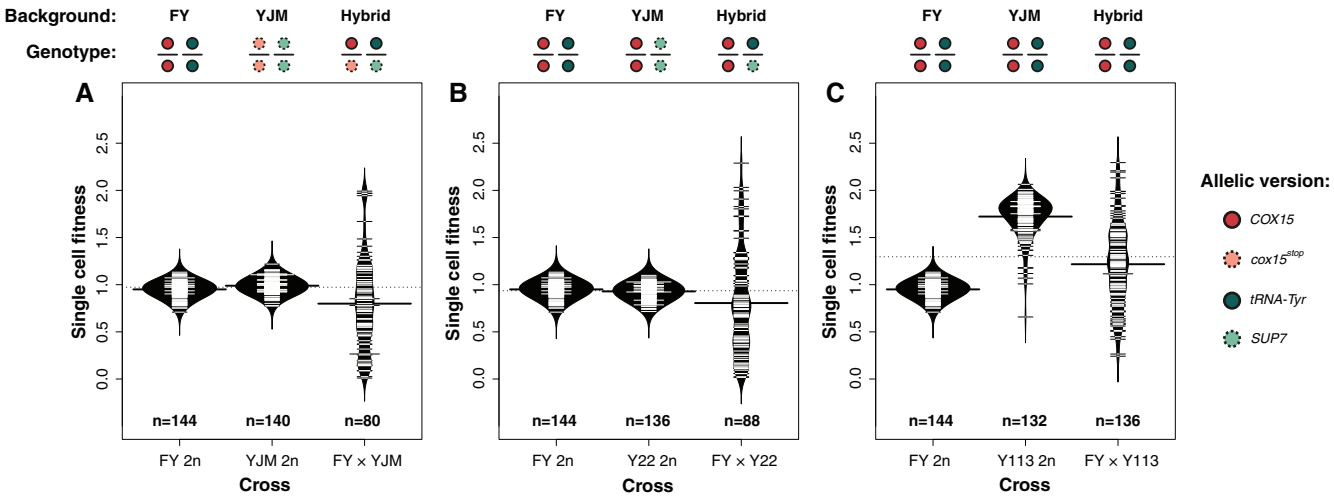

Fig. 1. Single cell fitness estimation using homozygous and hybrid backgrounds. Bean plots of offspring single cell fitness values are presented for different parental combinations as indicated. The number of full tetrad analyzed for each cross was indicated inside the panels. Different allelic versions at the *COX15* and *SUP7* loci are colour-coded. (*A*) Homozygous parental strains FY and YJM with the respective hybrid progeny. (*B*) Parental strains FY and Y22 with the respective hybrid progeny. (*C*) Parental strains FY and Y113 with the respective hybrid progeny.

the replacement of *cox15*^{stop} in the YJM background (fig. 1B). Moreover, the presence or absence of the *cox15*^{stop} allele showed little impact on the global fitness distribution pattern in the hybrid offspring (fig. 1B). Overall, these observations suggest that the *cox15*^{stop} do not play a major role in the tolerance of the suppressor.

Possible Trade-Offs between Fitness and Suppressor Tolerance

Once the effect of *cox15*^{stop} was eliminated by allele replacement, we sought to test the fitness impact of the suppressor in the YJM background by further replacing the *SUP7* allele with the corresponding wild type tyrosine tRNA tY(GUA)J1 (*tRNA-Tyr*). Intriguingly, the resulting strain Y113 (*COX15/tRNA-Tyr*) displayed a significant gain of fitness, which was nearly 2-fold higher than the lab strain FY (fig. 1C). The observed abnormal high fitness in the absence of *SUP7* clearly suggests a possible trade-off between growth and suppressor tolerance. In this scenario, the effect of the suppressor may be compensated by the high initial fitness level, which makes such individuals more robust to suppressor. In fact, when crossing the highly fit strain Y113 with FY, recombinant offspring presented a wide range of fitness variation, possibly leading to different potential of suppressor tolerance (fig. 1C).

Mapping of the Genes Involved in Suppressor Tolerance

To map the genomic loci underlying the observed high fitness and therefore suppressor tolerance, we generated a large segregating pool consisting of 1,200 offspring from the cross between Y113 and FY. We introduced the suppressor into the offspring using a plasmid carrying the *SUP7* allele under its native upstream regulatory region in YJM421, and selected a pool of 50 individuals with the lowest single cell fitness (fig. 2A). Segregants from the selected low fitness bulk were then independently cultured and pooled by equal cell density, and the resulting pool was subsequently sequenced using short reads strategy Illumina Hiseq with 50× coverage. The reads obtained were aligned to the genome of FY and the allele frequency was scored at each polymorphic position. For most genomic regions, the allele frequency of either parent is expected to be 0.5, whereas regions involved would show a skewed allele frequency. Using this strategy, we mapped two regions with a significant skewed allele frequency toward the nontolerant FY parent. The first region was found on chromosome XIV (position 441000–483000) and the second region on chromosome XV (position 553000–591000), spanning ~42 and 39 kb, respectively. By closely examining the mapped regions, we identified and focused on two candidate genes, namely *MKT1*, a master regulator involved in multiple cellular processes (chromosome XIV, 467131–469623) and *RGA1*, a putative GTPase activating protein related to cell polarization and septin organization (chromosome XV, 561170–564193) (fig. 2B and C). Both candidates harbored several nonsynonymous variations between the tolerant and nontolerant parents (supplementary table S3, Supplementary Material online). In addition, the YJM alleles for both candidates contained extremely rare nonsynonymous variations, with allele frequencies <5% across ~1,000 natural isolates of *S. cerevisiae* (supplementary table S3, Supplementary Material online; data obtained from the 1002 yeast genomes project, http://1002genomes.u-strasbg.fr). These observations further indicate that the observed the fitness outburst could be specific to the YJM background due to the presence of the suppressor.

Functional Validation of the Candidate Genes Using Quantitative Tetrad Analysis

To validate the effect of the candidate genes, we replaced individually each gene in the Y113 (*COX15/tRNA-Tyr*) background using the corresponding allelic version from the nontolerant FY parent. This resulted in two variant strains, namely Y113 *MKT1*Δ::*MKT1*^{FY} and Y113 *RGA1*Δ::*RGA1*^{FY}, which were otherwise identical to Y113, with the exception of the targeted loci. Both variants were crossed with Y113 to evaluate the fitness effect of the different allelic variations of the tolerant and nontolerant parents. To do so, we used a quantitative tetrad analysis strategy, which consists of evaluating the fitness distribution and segregation pattern of each meiotic event (tetrad) with *a priori* knowledge of the segregating loci in order to precisely estimate the fitness effects of different genotype combinations (fig. 3).

For the cross between Y113 *MKT1*Δ::*MKT1*^{FY} and Y113, a total of 34 full tetrads corresponding to 136 meiotic segregants were analyzed, resulting in a bimodal distribution of single cell fitness (fig. 3A). A maximum a posteriori (MAP) bimodal distribution model was fitted to the observed distribution data using a Expectation-Maximization (EM) algorithm, which allowed confident assignment of each individual into two fitness clusters with equal proportions (0.493 vs. 0.506) (fig. 3A). We observed a 2:2 segregation pattern for the lower versus higher fitness clusters in the tetrads, consisting with the expectation of a single segregating locus. The fitness level of the parental strain Y113 was previously known, corresponding to the higher fitness cluster (mean = 1.926) (fig. 3A). As a result, the mean fitness of Y113 *MKT1*Δ::*MKT1*^{FY} can be deduced as the mean of the lower fitness cluster (mean = 1.115) (fig. 3A). This observation showed that the YJM version of *MKT1* indeed contributes to higher fitness compare to *MKT1*^{FY}in the absence of the suppressor.

To test the effect of the *MKT1* alleles in combination with the suppressor *SUP7*, we crossed Y113 *MKT1*Δ::*MKT1*^{FY} to Y22 and analyzed the fitness distribution of the resulting offspring (fig. 3B). Under Mendelian segregation, we would expect four types of genotypic combinations, namely *MKT1*^{YJM}/*tRNA-Tyr*, *MKT1*^{YJM}/*SUP7*, *MKT1*^{FY}/*tRNA-Tyr* and *MKT1*^{FY}/*SUP7*, each with equal proportions. As the mean fitness values of the first three genotype combinations were known, each corresponding to Y113, Y22, Y113 *MKT1*Δ::*MKT1*^{FY}, respectively, the fitness effect of *MKT1*^{FY}/*SUP7* can be deduced. In total, 33 full tetrads (132 spores) were analyzed, leading to a trimodal distribution pattern (fig. 3B). The relative proportion of the lower, intermediate and higher fitness clusters were 0.328, 0.409 and 0.262, as expected from a two loci segregating model providing that the genotype combinations *MKT1*^{YJM}/*SUP7* and *MKT1*^{FY}/*tRNA-Tyr*

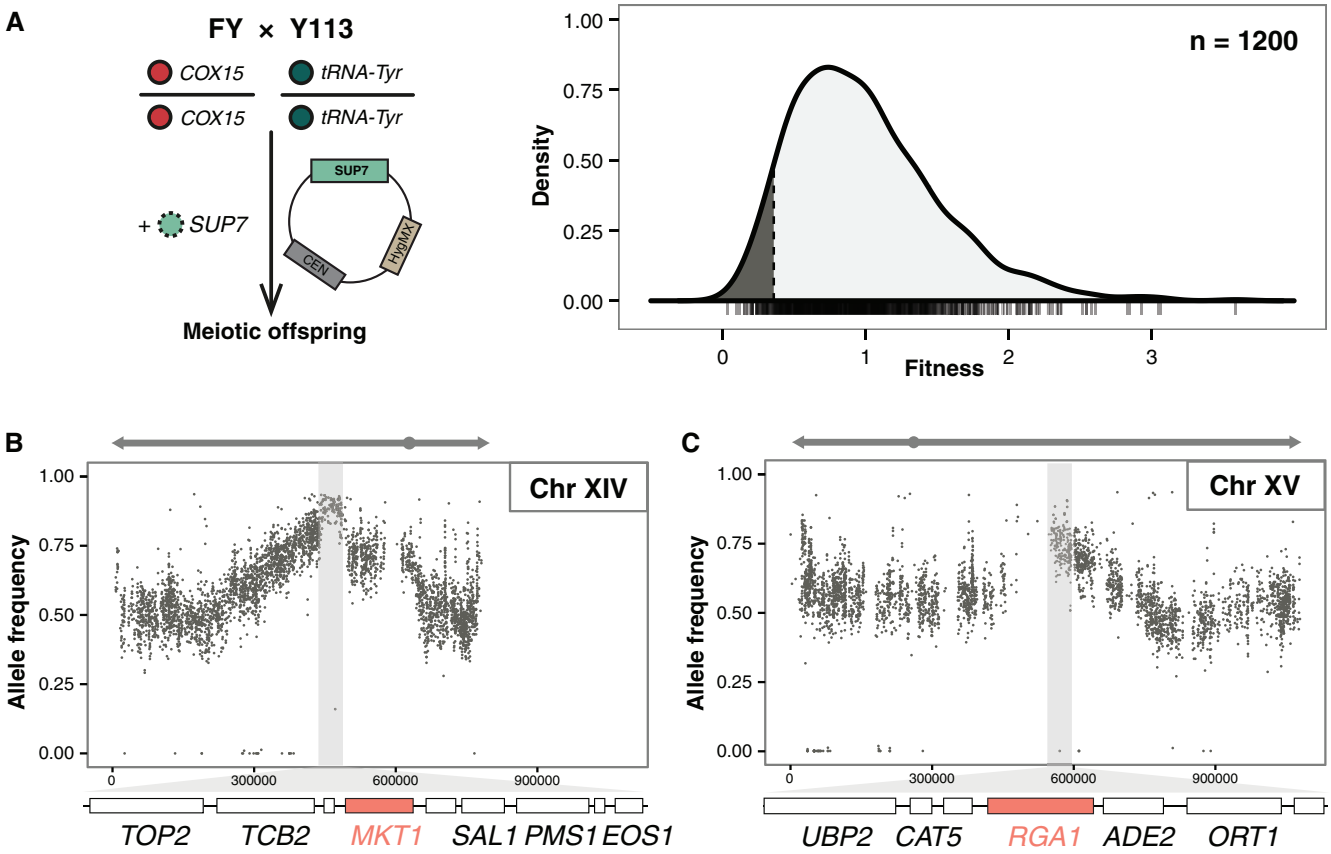

FIG. 2. Bulk segregant analysis identified loci involved in suppressor tolerance. (*A*) The scheme of experimental design was indicated at the left panel. In total, 1,200 segregants originated from the FY/Y113 cross were analyzed, and 50 segregants with the lowest fitness in the presence of the suppressor *SUP7* were retained. The resulting pool was sequenced and the regions involved were identified by looking at allele frequency variation. (*B*) Identified region on chromosome XIV (position 441000–483000). Region with the most enriched allele frequency for the nontolerant FY parent was represented as the shaded area. Genes presented in this region were schematized and the candidate gene was highlighted. (*C*) Identified region on chromosome XV (position 553000–591000) with the same representation. See supplementary table S1, Supplementary Material online, for nonsynonymous nucleotide changes between the parental alleles of *MKT1* and *RGA1*.

display equivalent fitness levels. Indeed, the fitness levels of $MKT1^{YJM}$/*SUP7* and $MKT1^{FY}$/*tRNA-Tyr* were comparable, with mean fitness of 1.063 and 1.115, respectively. Therefore, the mean fitness value of the $MKT1^{FY}$/*SUP7* corresponded to the lower cluster mean (mean = 0.688). These results validated the role of *MKT1* in the suppressor tolerance, where the allele from the nontolerant FY parent leads to significant fitness loss both individually or in combination with the suppressor (fig. 4*A*).

The same procedures were carried out for the candidate *RGA1* gene. We observed again a bimodal distribution with 2:2 tetrad segregation in the offspring originated from crossing Y113 *RGA1*Δ::$RGA1^{FY}$ with Y113 (35 full tetrads), leading to deduced fitness level of Y113 *RGA1*Δ::$RGA1^{FY}$ at 1.266 (fig. 3*C*). Offspring resulting from a cross between Y113 *RGA1*Δ::$RGA1^{FY}$ and Y22 led to a trimodal distribution, with relative proportions of the lower, intermediate and higher fitness clusters corresponding to 0.283, 0.478 and 0.238 (fig. 3*D*). Using the same principle, the fitness value of the genotype combination $RGA1^{FY}$/*SUP7* was estimated as the mean of the lower fitness cluster (mean = 0.691).

By calculating the cumulative mean and SD from the quantitative tetrad distributions (fig. 3), we estimated the fitness outcomes of different genotypic combinations in the YJM background (fig. 4). The results clearly showed that the YJM alleles of both *MKT1* and *RGA1* genes contribute to higher fitness, allowing a better tolerance of the *SUP7* suppressor compared with the allelic versions from the nontolerant FY parent (fig. 4). In the case of *MKT1*, the YJM version contributes to a 1.6-fold increase of fitness in the presence of *SUP7*, with cumulative mean of 1.081 ($MKT1^{YJM}$/*SUP7*, SD = 0.232) versus 0.688 ($MKT1^{FY}$/*SUP7*, SD = 0.123) (fig. 4*A*). For *RGA1*, a 1.6-fold increase of fitness was also observed, with the YJM version contributing to a mean fitness of 1.104 ($RGA1^{YJM}$/*SUP7*, SD = 0.169) versus 0.690 ($RGA1^{FY}$/*SUP7*, SD = 0.060) (fig. 4*B*).

Additive Contribution of the Identified Alleles Explains the Observed Fitness Variation

To test the combined effect of the identified alleles, we crossed Y113 *MKT1*Δ::$MKT1^{FY}$ with Y113 *RGA1*Δ::$RGA1^{FY}$, leading to a diploid strain heterozygous for both *MKT1* and *RGA1* in the YJM background. Curiously, the resulting diploid showed sporulation deficiency, possibly due to interactions with other variants specific to this genetic background. To circumvent this problem, we performed

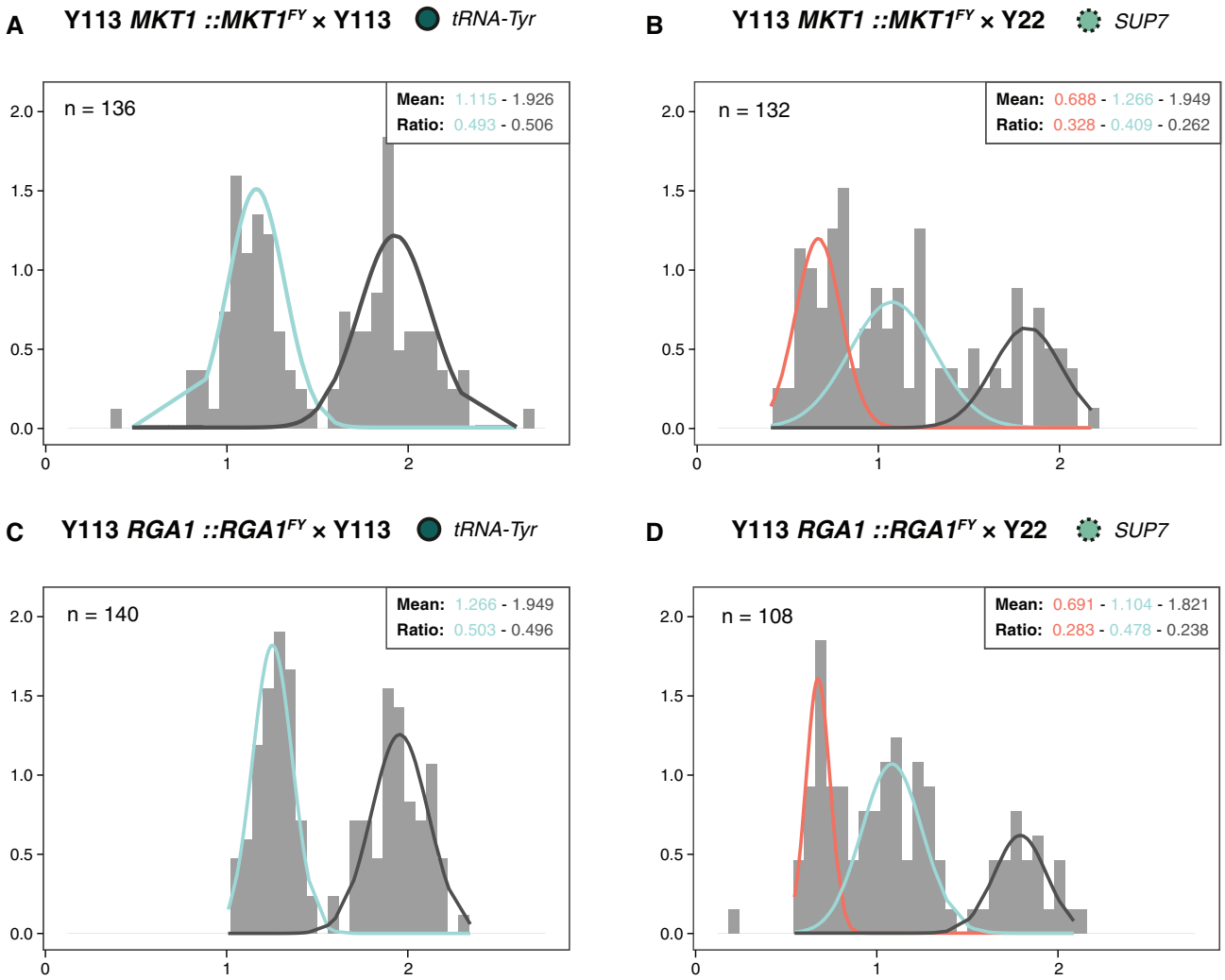

Fig. 3. Quantitative tetrad analyses using single cell fitness distribution. Offspring fitness distribution patterns for crosses with various genotypic combinations as indicated. *A priori* bimodal (*A* and *C*) and trimodal (*B* and *D*) distribution models were applied using Expectation Maximization algorithm. Fitted clusters are colour-coded, and the respective mean and ratio of each detected cluster were indicated at the upper right position. The number of segregant analyzed in each cross was indicated at upper left. (*A*) Offspring fitness distribution from the cross between Y113 *MKT1*Δ::*MKT1*^{FY}and Y113. (*B*) Cross between Y113 *MKT1*Δ::*MKT1*^{FY}and Y22. (*C*) Cross between Y113 *RGA1*Δ::*RGA1*^{FY}and Y113. (*D*) Cross between Y113 *RGA1*Δ::*RGA1*^{FY}and Y22. Single cell fitness levels are shown on the *x*-axis, with binned densities on the *y*-axis.

a simulation study by integrating the genotypic effects previously inferred using quantitative tetrad analyses for both genes under an additive model (fig. 5*A*). The simulated data were then compared with the single cell fitness distribution observed for offspring originated from the cross between FY and Y113, a hybrid background heterozygous for *MKT1* and *RGA1* (fig. 5*B*). In this case, if *MKT1* and *RGA1* act additively, we expect similar distribution patterns in the simulation compared with the FY × Y113 hybrid, assuming the fitness effects of the YJM alleles were equally valid in both backgrounds. Whereas in the case of nonadditive genetic interactions, a deviation of the distribution may be observed.

In fact, by comparing the simulated data with the observed distribution in the FY × Y113 hybrid, we observed similar patterns with the same mean fitness values (1.206 vs. 1.243, Welch two sample *t*-test, *P* value = 0.417) and conserved variances (*F* test, *P* value = 0.0004). These data indicate that the YJM alleles of *MKT1* and *RGA1* contribute to the observed fitness gain additively, with similar effects in both the YJM and FY backgrounds.

Discussions

Cellular Energy Production, Homeostasis and Suppressor Tolerance

Using single cell fitness assays, quantitative tetrad analyses and allele replacements, we identified and validated two genes, namely *MKT1* and *RGA1*, which were involved in the observed suppressor tolerance. We precisely estimated the fitness outcomes of different genotypic combinations relative to the presence or absence of *SUP7*. We showed that YJM allelic variants of both genes confer a fitness advantage compared with the corresponding alleles of the nontolerant FY

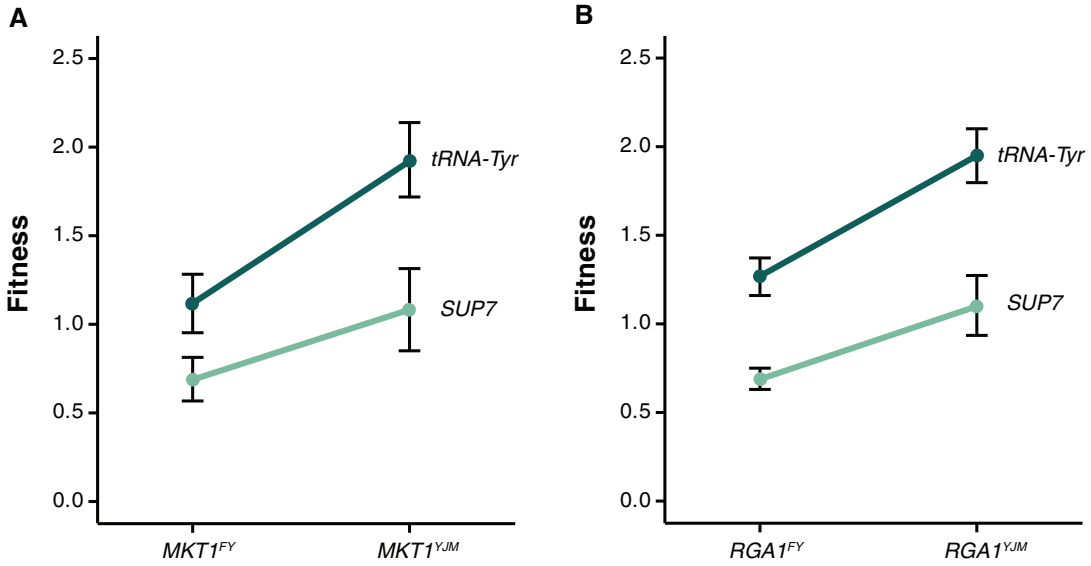

Fig. 4. Genotypic values related to different allelic combinations of *MKT1*, *RGA1* and *SUP7*. (*A*) Cumulative mean and SD deduced from quantitative tetrad analyses for the loci *MKT1* and *SUP7*. $MKT1^{YJM}$/*tRNA-Tyr*: mean = 1.926; SD = 0.210. $MKT1^{YJM}$/*SUP7*: mean = 1.081; SD = 0.232. $MKT1^{FY}$/*tRNA-Tyr*: mean = 1.115; SD = 0.165. $MKT1^{FY}$/*SUP7*: mean = 0.688; SD = 0.123. (*B*) Cumulative mean and SD deduced from quantitative tetrad analyses for the loci *RGA1* and *SUP7*. $RGA1^{YJM}$/*tRNA-Tyr*: mean = 1.949; SD = 0.152. $RGA1^{YJM}$/*SUP7*: mean = 1.104; SD = 0.169. $RGA1^{FY}$/*tRNA-Tyr*: mean = 1.266; SD = 0.106. $RGA1^{FY}$/*SUP7*: mean = 0.690; SD = 0.060.

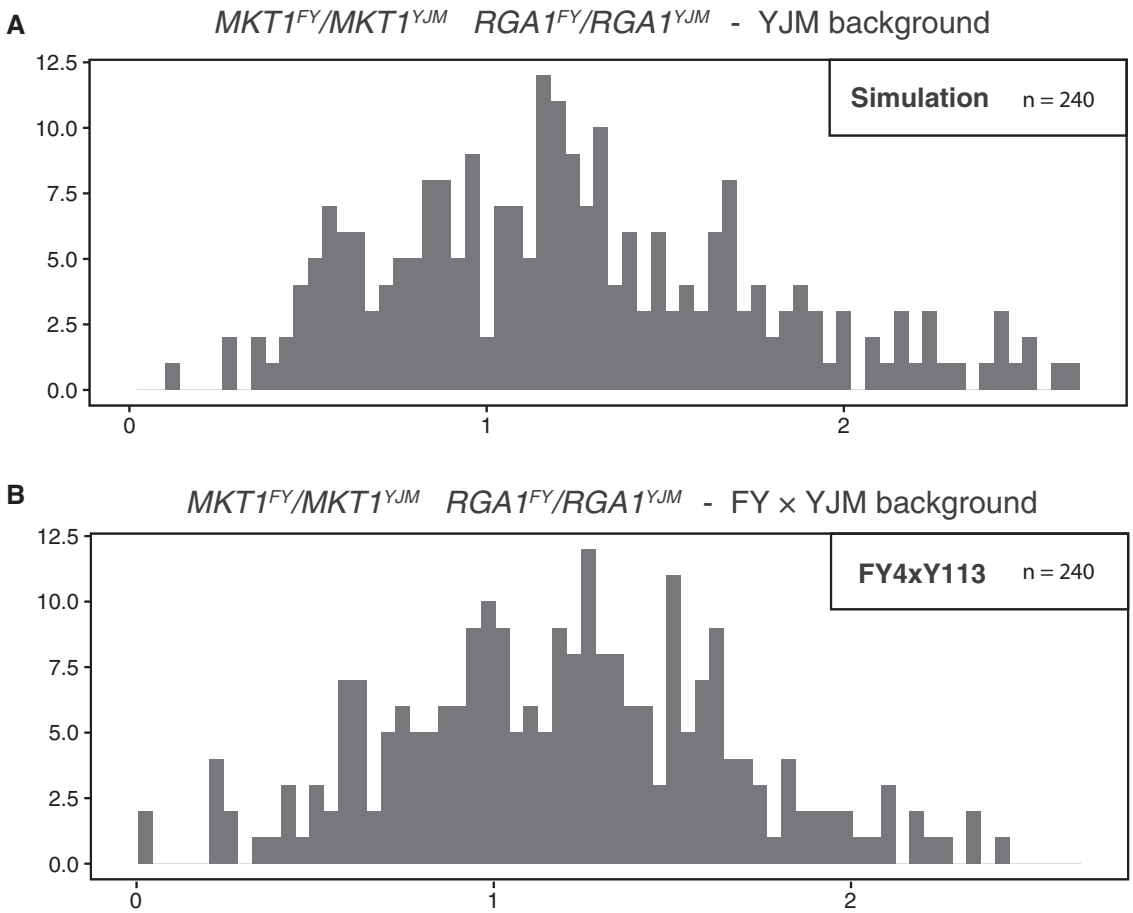

Fig. 5. Comparison of single cell fitness distribution using simulation data under additive model. (*A*) Simulated fitness distribution under additive model for heterozygous $MKT1^{FY}/MKT1^{YJM}$ and $RGA1^{FY}/RGA1^{YJM}$ in the YJM background for 240 individuals from full tetrads. (*B*) Observed distribution for 240 individuals from full tetrads originated from hybrid between FY and Y113.

strain, possibly suggesting an allele-specific dysregulation of cellular energy production and homeostasis.

At the functional level, both *MKT1* and *RGA1* could potentially be important to internal proteomic stress. Null mutants of both *MKT1* and *RGA1* could display reduced respiratory potential, altered protein distributions and overall decrease of mitotic fitness (Smith and Kruglyak 2008; Anderson et al. 2010; Meitinger et al. 2013; Samanfar et al. 2013). Notably, *MKT1* has been repeatedly found to be involved in a wide-range of stress related phenotypes in *S. cerevisiae* such as ethanol resistance, heat tolerance, oxidative stress (Steinmetz et al. 2002; Swinnen et al. 2012; Lewis et al. 2014; Treusch et al. 2015). It has been shown that *MKT1* encodes for a master transcriptional regulator, displaying pleiotropic effect on a large number of cellular processes through transcriptomic reorganization (Brem and Kruglyak 2005). The extensive pleiotropy of *MKT1* could make it a favourable target for phenotypic diversity (Fay 2013). Indeed, adding to the existing list of phenotypic impacts, here we showed that *MKT1* could also confer tolerance to tRNA nonsense suppressor through fitness trade-offs. Nevertheless, the precise molecular basis underlying this particular phenotype is still unclear.

Fitness Trade-Offs and Adaptive Potential in Yeast Natural Populations

Despite a fitness cost on rich media, carrying a tRNA suppressor may offer some adaptive advantages in stress environments depending on genetic backgrounds (Hou et al. 2015). Possibly by exposing previously inaccessible genomic variation such as genes with nonsense mutations, tRNA suppressors could confer increased phenotypic variance in a large number of stress conditions in a background specific manner (Hou et al. 2015). In fact, by surveying 100 genomes of *S. cerevisiae* (Strope et al. 2015), we previously showed a relatively high frequency of nonsense mutations across natural populations, ranging from 18 to 49 nonsense mutation per isolate with an average of ~10 in each stop codon class (Hou et al. 2015). Such conditionally neutral variants constitute a reservoir for phenotypic novelty in the presence of tRNA suppressors. However, contrasting to the commonplace of nonsense mutations, the frequency of suppressors across the species is exceedingly low, with the *SUP7* allele as the only tRNA suppressor of any stop codon class identified so far. Hence, tRNA suppressors might represent a transient mechanism, which could subsequently be lost in the absence of selection. Moreover, the rarity of such suppressors may arguably be attributed to a fitness cost due to excessive read-through of native stop codons, which leads to internal proteomic stress (Torabi and Kruglyak 2012).

Interestingly, many mechanisms involved in rapid stress responses, such as aneuploidies, may present similar internal stress effects. Aneuploidies alter gene dosage at the chromosomal scale. Such dosage imbalance could confer rapid adaptation to stress conditions by amplifying advantageous genes and alleles, but could also lead to internal proteomic stress. While it has been shown that aneuploidies could have large fitness costs, the tolerance of aneuploidies varies across different genetic backgrounds, especially in various natural isolates (Hose et al. 2015). Another extensively studied example of trade-offs between fitness and internal proteomic stress involved the yeast prion [PSI^+], the effect of which could be inherently similar to tRNA suppressors (Halfmann et al. 2012). [PSI^+] induced stop codon read-through can trigger Hsp90p related stress responses, hallmark of proteomic perturbations (Halfmann et al. 2012).

It is intriguing that multiple mechanisms with inherent fitness cost may often offer selective advantages when challenged by stress. More importantly, the fitness cost could be leveraged by intrinsic genomic variation related to different genetic backgrounds, possibly resulting in individual variability in adaptive potential. However, contrasting to aneuploidies or prions, tRNA suppressors in natural populations of yeast are rare (1/100), albeit potentially presenting similar phenotypic effects. Further exploring the YJM421 isolate, a unique background that tolerate the suppressor, at the system level by integrating global genomic, transcriptomic and proteomic information would certainly be interesting to offer new evolutionary insights into the basis of trade-offs between fitness and adaptive potential.

Materials and Methods

Strains

Laboratory strains FY4 (*MAT*a), FY5 (*MAT*a) isogenic to S288c were used. Strain variants in the YJM421 background were generated using 5-FOA selection as previously described (Hou et al. 2015), and subsequently backcrossed to the original YJM421 strain to eliminate the Δ*ura3* auxotrophic marker. An additional round of backcross was performed to ensure genomic homogeneity. Detailed genotypes for strains used in this study are listed in supplementary table S1, Supplementary Material online. A complete genealogical relationship of the strains generated is shown in supplementary figure S1, Supplementary Material online. All genotypes were confirmed using PCR, and primers used are listed in supplementary table S2, Supplementary Material online.

Media and Culture Conditions

All growth and fitness assays were carried on standard rich media YPD (1% yeast extract, 2% peptone and 2% glucose). YPD media containing 200 μg/ml hygromycin were used to maintain plasmid selection. Sporulation was induced on potassium acetate plates (1% potassium acetate, 2% agar). All procedures were performed at 30 °C.

Single Cell Fitness Assay

To measure single cell fitness, diploid cells were sporulated and the resulting tetrads were dissected using MSM 400 micromanipulator (Singer instrument) after digestion of the asci using zymolyase (MP Biomedicals). Each dissection plate contains 20 tetrads with individual spores aligned on a 9×10 matrix. For each plate, a total of 10 individual cells isolated from an exponentially growing YPD culture of FY5 were aligned to the matrix as intra-plate control. The resulting

dissection plates were culture at 30 °C for 48 h, and then scanned at a resolution of 600 dpi. Colony size for each individual was calculated using the R package Gitter (Wagih and Parts 2014), with customized 9 × 10 plate format. Single cell fitness values were calculated by normalizing the colony size of the tested strain with the average colony size of the control cells. All analyses were performed in R.

Bulk Segregant Analysis

In total, 50 individuals with the lowest fitness values in the presence of the suppressor *SUP7* from the cross between FY and Y113 were selected and independently cultured in YPD overnight, then pooled by equal cell density (O.D readings at 600 nm). The DNA of the pool was extracted using 100/G columns and Genomic DNA buffers (QIAGEN) as described previously (Hou et al. 2014). After whole genome sequencing, the genomic regions involved were identified by looking at allele frequency variation.

Genotyping Strategy and Data Treatment

DNA sequencing was performed using Illumina Hiseq 2000. We used paired-end libraries, 101 bp/read, with 50× coverage. Reads were mapped to the FY genome using BWA with "-n 5 -o 2" options (Li et al. 2009). Single nucleotide polymorphism (SNP) calling was performed using SAMtools (Li et al. 2009), with default parameters. The allele frequency of FY was calculated for each polymorphic position along the genome. A value of allele frequency equals to 1 indicates all individuals in the segregant pool possessed the allelic version of FY.

Model Fitting and Calculation of the Fitness Effect of Genotype Combinations

For each single cell fitness distribution, an *a priori* distribution model was fitted using the R package "mixtools" (https://cran.r-project.org/web/packages/mixtools/index.html) with $k = 2$ for single segregating locus and $k = 3$ for two segregating loci. Mean, SD, and proportion of each cluster were extracted from the output file. Posterior probability (PP) for each individual and each cluster was also extracted, and a cutoff of $PP > 0.9$ was applied for cluster assignment in bimodal distribution cases. For each genotype combination, mean fitness values were calculated as the pooled mean and SD from independent crosses with the corresponding fitness cluster, using the formula below:

$$\mu_{pooled} = \frac{\sum_{i=1}^{x} \mu_i \times n_i}{\sum_{i=1}^{x} n_i}$$

$$sd_{pooled} = \sqrt{\frac{\sum_{i=1}^{x} ((n_i - 1) \times sd_i)^2}{\sum_{i=1}^{x} n_i - x}}$$

Where x is the number of independent measurements, μ is the observed mean fitness value for the cluster corresponding a given genotype combination, and SD is the standard deviation from each measurements. All analyses were performed in R.

Simulation of Fitness Distributions

Simulation of the single cell fitness distributions was performed in R. A two by four matrix was generated to simulate segregation of two independent loci in a given tetrad. Genotypic values of the *MKT1* and *RGA1* alleles were randomly sampled from a normal distribution of 100 individual simulated using the cumulative mean and SDs calculated previously. The sampled values were filled in the matrix as a 2:2 segregation. The matrix is then randomized by each column of four randomly segregating 2:2 alleles, and the fitness value for each individual was calculated as the multiplicative value of each row, representing the alleles for both loci. In total, 60 full tetrads were simulated representing 240 meiotic individuals.

Supplementary Material

Supplementary figure S1 and tables S1–S3 are available at *Molecular Biology and Evolution* online .

Acknowledgments

This study was supported by National Institutes of Health (NIH Grant R01 GM101091-01) and the Agence Nationale de la Recherche (ANR Grant 2011-JSV6-004-01). J.H. is supported in part by a grant from the Ministère de l'Enseignement Supérieur et de la Recherche and in part by a fellowship from the medical association La Ligue contre le Cancer.

References

Anderson JB, Funt J, Thompson DA, Prabhu S, Socha A, Sirjusingh C, Dettman JR, Parreiras L, Guttman DS, Regev A, et al. 2010. Determinants of divergent adaptation and Dobzhansky-Muller interaction in experimental yeast populations. *Curr Biol.* 20:1383–1388.

Bergstrom A, Simpson JT, Salinas F, Barre B, Parts L, Zia A, Nguyen Ba AN, Moses AM, Louis EJ, Mustonen V, et al. 2014. A high-definition view of functional genetic variation from natural yeast genomes. *Mol Biol Evol.* 31:872–888.

Brem RB, Kruglyak L. 2005. The landscape of genetic complexity across 5,700 gene expression traits in yeast. *Proc Natl Acad Sci U S A.* 102:1572–1577.

Chang SL, Lai HY, Tung SY, Leu JY. 2013. Dynamic large-scale chromosomal rearrangements fuel rapid adaptation in yeast populations. *PLoS Genet.* 9:e1003232.

Dunham MJ, Badrane H, Ferea T, Adams J, Brown PO, Rosenzweig F, Botstein D. 2002. Characteristic genome rearrangements in experimental evolution of *Saccharomyces cerevisiae*. *Proc Natl Acad Sci U S A.* 99:16144–16149.

Fay JC. 2013. The molecular basis of phenotypic variation in yeast. *Curr Opin Genet Dev.* 23:672–677.

Gresham D, Desai MM, Tucker CM, Jenq HT, Pai DA, Ward A, DeSevo CG, Botstein D, Dunham MJ. 2008. The repertoire and dynamics of evolutionary adaptations to controlled nutrient-limited environments in yeast. *PLoS Genet.* 4:e1000303.

Halfmann R, Alberti S, Lindquist S. 2010. Prions, protein homeostasis, and phenotypic diversity. *Trends Cell Biol.* 20:125–133.

Halfmann R, Jarosz DF, Jones SK, Chang A, Lancaster AK, Lindquist S. 2012. Prions are a common mechanism for phenotypic inheritance in wild yeasts. *Nature* 482:363–368.

Hose J, Yong CM, Sardi M, Wang Z, Newton MA, Gasch AP. 2015. Dosage compensation can buffer copy-number variation in wild yeast. *Elife* 4:e05462.

Hou J, Friedrich A, de Montigny J, Schacherer J. 2014. Chromosomal rearrangements as a major mechanism in the onset of reproductive isolation in *Saccharomyces cerevisiae*. *Curr Biol.* 24:1153–1159.

Hou J, Friedrich A, Gounot JS, Schacherer J. 2015. Comprehensive survey of condition-specific reproductive isolation reveals genetic incompatibility in yeast. *Nat Commun.* 6:7214.

Lewis JA, Broman AT, Will J, Gasch AP. 2014. Genetic architecture of ethanol-responsive transcriptome variation in *Saccharomyces cerevisiae* strains. *Genetics* 198:369–382.

Li H, Handsaker B, Wysoker A, Fennell T, Ruan J, Homer N, Marth G, Abecasis G, Durbin R. 2009. The Sequence Alignment/Map format and SAMtools. *Bioinformatics* 25:2078–2079.

Liebman SW, Sherman F. 1976. Inhibition of growth by amber suppressors in yeast. *Genetics* 82:233–249.

Meitinger F, Richter H, Heisel S, Hub B, Seufert W, Pereira G. 2013. A safeguard mechanism regulates Rho GTPases to coordinate cytokinesis with the establishment of cell polarity. *PLoS Biol.* 11:e1001495.

Samanfar B, Omidi K, Hooshyar M, Laliberte B, Alamgir M, Seal AJ, Ahmed-Muhsin E, Viteri DF, Said K, Chalabian F, et al. 2013. Large-scale investigation of oxygen response mutants in *Saccharomyces cerevisiae*. *Mol Biosyst.* 9:1351–1359.

Skelly DA, Merrihew GE, Riffle M, Connelly CF, Kerr EO, Johansson M, Jaschob D, Graczyk B, Shulman NJ, Wakefield J, et al. 2013. Integrative phenomics reveals insight into the structure of phenotypic diversity in budding yeast. *Genome Res.* 23:1496–1504.

Smith EN, Kruglyak L. 2008. Gene-environment interaction in yeast gene expression. *PLoS Biol.* 6:e83.

Steinmetz LM, Sinha H, Richards DR, Spiegelman JI, Oefner PJ, McCusker JH, Davis RW. 2002. Dissecting the architecture of a quantitative trait locus in yeast. *Nature* 416:326–330.

Strope PK, Skelly DA, Kozmin SG, Mahadevan G, Stone EA, Magwene PM, Dietrich FS, McCusker JH. 2015. The 100-genomes strains, an *S. cerevisiae* resource that illuminates its natural phenotypic and genotypic variation and emergence as an opportunistic pathogen. *Genome Res.* 25:762–774.

Swinnen S, Schaerlaekens K, Pais T, Claesen J, Hubmann G, Yang Y, Demeke M, Foulquie-Moreno MR, Goovaerts A, Souvereyns K, et al. 2012. Identification of novel causative genes determining the complex trait of high ethanol tolerance in yeast using pooled-segregant whole-genome sequence analysis. *Genome Res.* 22:975–984.

Torabi N, Kruglyak L. 2012. Genetic basis of hidden phenotypic variation revealed by increased translational readthrough in yeast. *PLoS Genet.* 8:e1002546.

Treusch S, Albert FW, Bloom JS, Kotenko IE, Kruglyak L. 2015. Genetic mapping of MAPK-mediated complex traits across *S. cerevisiae*. *PLoS Genet.* 11:e1004913.

True HL, Lindquist SL. 2000. A yeast prion provides a mechanism for genetic variation and phenotypic diversity. *Nature* 407:477–483.

Wagih O, Parts L. 2014. gitter: a robust and accurate method for quantification of colony sizes from plate images. *G3 (Bethesda)* 4:547–552.

Warringer J, Zorgo E, Cubillos FA, Zia A, Gjuvsland A, Simpson JT, Forsmark A, Durbin R, Omholt SW, Louis EJ, et al. 2011. Trait variation in yeast is defined by population history. *PLoS Genet.* 7:e1002111.

Yona AH, Manor YS, Herbst RH, Romano GH, Mitchell A, Kupiec M, Pilpel Y, Dahan O. 2012. Chromosomal duplication is a transient evolutionary solution to stress. *Proc Natl Acad Sci U S A.* 109:21010–21015.